

## 3D-QSAR studies of xanthone derivatives as human alpha glucosidase inhibitors

Uzma Saqib, Mohammad Imran Siddiqi \*

Molecular and Structural Biology Division, Central Drug Research Institute, Lucknow, India

Submitted: 13 Oct. 2008; Accepted: 30 Dec. 2008

### Abstract

Three-dimensional quantitative structure activity relationship (3D-QSAR) analyses were carried out on a set of 42 xanthone derivatives in order to understand their anti-alpha glucosidic activities. The studies include Comparative Molecular Field Analysis (CoMFA) and Comparative Molecular Similarity Indices Analysis (CoMSIA). Models with good predictive abilities were generated with the cross validated  $r^2$  ( $r^2_{cv}$ ) values for CoMFA and CoMSIA being 0.580 and 0.610 respectively. The conventional  $r^2$  values were 0.949 each for both CoMFA and CoMSIA models. In addition, a homology model of human alpha glucosidase was used for docking based alignment of the compounds. The most active compound then served as a template for the alignment of the remaining structures in order to align all compounds prior to QSAR studies. Further, mapping of contours onto the active site validated each other in terms of residues involved with reference to respective contours. This integrated molecular docking based alignment followed by 3D-QSAR studies should provide further insights to support structure-based design of anti-diabetic agents with improved activity profiles.

**Keywords:** Type 2 Diabetes mellitus, Xanthenes, Human alpha glucosidase, CoMFA, CoMSIA.

## INTRODUCTION

Type2 diabetes is one of the major life threatening disease all over the world. Its cases are progressing at an incremental rate every year (World Health Organisation Fact Sheet No. 312.,2008 ; International Diabetes Federation., 2006; Boehringer Ingelheim. Annual Report, 2007). In spite of the latest advances in drug discovery process there has been no 'fully potent-no side effect' drug appeared in the market. Previously, while due to no well defined molecular targets or lack of understanding of disease pathophysiology, treatment of type2 diabetes was mostly focused on insulin secretion or administration of external insulin. During the past decade however, advent of genomics and proteomics has helped in understanding the molecular alteration characteristics of NIDDM (Das *et al.*, 2005). Currently, various approaches are present to curb the disease. Among these, inhibition of alpha glucosidase is one. Alpha-glucosidase (EC 3.2.1.20) catalyzes the final step in the digestion of carbohydrates (Robinson *et al* 1991; Braun *et al.*, 1995; Dwek *et al.*, 2002).

Inhibitors of the enzyme may retard the uptake of dietary carbohydrates and suppress postprandial hyperglycemia, and may therefore have considerable potential for the treatment of various diseases, including diabetes, certain forms of hyperlipoproteinemia, and obesity. (Truscheit *et al.*,1981; Madariaga *et al.*,1998; Lajola *et al.*,1984; McCulloch *et al.*,1983). There has been reports of plenty of alpha glucosidase inhibitors [Melo *et al.*, 2006; Gao *et al.*, 2005; Matsuura *et al.*, 2004; Hai-Wei *et al.*, 2007). Some inhibitors like acarbose, miglitol and voglibose are already in market. However, there is still a need of more potent inhibitors which can strongly inhibit the enzyme. As yet, no report has been published regarding the 3-D QSAR studies of the alpha glucosidase inhibitors. Here, we present the first QSAR studies of inhibitors of alpha glucosidase. In the present study, 3D-QSAR analyses were carried out on the series of xanthone derivatives as alpha glucosidase inhibitors in order to identify the key structural elements required to design potential drug candidates of this class. The studies include common substructure-based alignment of compounds based on the docked conformation of most active compound of the series followed by CoMFA (Cramer *et al.*, 1988) and CoMSIA (Klebe *et al.*, 1994) analysis. Furthermore, the results of the QSAR model were mapped upon the protein binding site which further validated the contour maps with reference to corresponding residues in the

### \*Corresponding author:

Mohammad Imran Siddiqi, Ph.D.  
Molecular and Structural Biology Division,  
Central Drug Research Institute,  
Lucknow 226 001, India  
Email: imsiddiqi@yahoo.com

binding site and thus helped in understanding ligand–receptor interactions through structure-based studies.

The contour maps derived from both the CoMFA and CoMSIA models permitted an understanding of the steric, electrostatic, lipophilic and hydrogen bonding requirements for ligand binding. As a consequence, the structural variations in the training set that give rise to variations in the molecular fields at particular regions of the space are correlated to biological activities serving as a guide to the design of novel inhibitors. The results obtained from this study would be useful in both understanding the favorable and non-favorable contours as well as in rapidly and accurately predicting the activities of newly designed inhibitors. These models also provide some beneficial clues in structural modification for designing new inhibitors for the treatment of Type2 Diabetes with much improved inhibitory activities against alpha glucosidase.

## MATERIALS AND METHODS

### Molecular structures and optimization

Forty two molecules selected for the present study were taken from the earlier reported work (Liu *et al.*, 2006; Liu *et al.*; 2007; Seo *et al.*, 2007). The structures of the compounds and their biological data are given in Table 1 [Supplementary data]. The IC<sub>50</sub> values were converted to the corresponding pIC<sub>50</sub> (-logIC<sub>50</sub>) and used as dependent variables in CoMFA and CoMSIA analysis. The pIC<sub>50</sub> values span a range of 3-log units providing a broad and homogenous data set for 3D-QSAR study. The 3D QSAR models were generated using a training set of 34 molecules. Predictive power of the resulting models was evaluated using a test set of 8 molecules (Table 1 marked with \*). The test compounds were selected manually such that the structural diversity and wide range of activity in the data set were included.

### Molecular alignment

**FlexX docking:** An already reported structure model of human alpha glucosidase (Saqib *et al.*, 2008) was used for the docking studies. In the current study, we docked all the 42 compounds into the binding site of homology modeled protein. The docking was performed with FlexX program (Rarey *et al.*, 1996). Ligands were docked into the ligand binding site with hydrogens present, and formal charges were assigned by FlexX. The best scoring conformation was chosen among the resulting 30 docking solutions.

CoMFA results may be extremely sensitive to a number of factors such as alignment rules, over all orientation of the aligned compounds, lattice shifting step size and probe atom type (Cho *et al.*, 1995). Often, similar functional groups or common atoms are chosen as alignment points to determine how compounds will

overlap. Docking ligands to a receptor has also been employed as a rationale for alignment. In the present study we used a combination of these methods by first solving the theoretical alpha glucosidase-bound conformations of all the compounds and then further fitting all the compounds on the docked conformation of the most active compound **28** as an alignment template using a common substructure with the SYBYL routine database align.

### CoMFA studies

Partial atomic charges were calculated using the Gasteiger-Huckel method. Steric and electrostatic interactions were calculated using the Tripos force field (Clark *et al.*, 1989) with a distance-dependent dielectric constant at all interactions in a regularly spaced (2Å) grid taking a sp<sup>3</sup> carbon atom as steric probe and a +1 charge as electrostatic probe. The cutoff was set to 30kcal/mol. With standard options for scaling of variables, the regression analysis was carried out using the full cross-validated partial least squares (PLS) (Stahle *et al.*, 1988) method (leave one out). The minimum sigma (column filtering) was set to 2.0kcal/mol to improve the signal to noise ratio by omitting those lattice points whose energy variation was below this threshold. The final model, non cross-validated conventional analysis was developed with the optimum number of components to yield a non cross-validated r<sup>2</sup> value.

### CoMSIA studies

Partial atomic charges were calculated using the MMFF94 method. In CoMSIA, a distance-dependent Gaussian-type physicochemical property has been adopted to avoid singularities at the atomic positions and dramatic changes of potential energy for those grids in the proximity of the surface. With the standard parameters and no arbitrary cutoff limits, three physicochemical properties, that is, steric, electrostatic and hydrophobic fields were calculated. The steric contribution was reflected by the third power of the atomic radii of the atoms. Electrostatic properties were introduced as atomic charges resulted from molecular docking. An atom-based hydrophobicity was assigned (Gohlke *et al.*, 2000; Viswanadhan *et al.*, 1989). The lattice dimensions were selected with a sufficiently large margin (>4Å) to enclose all the binding conformations of the inhibitors. In general, similarity indices, A<sub>F,K</sub> between the compounds of interest were computed by placing a probe atom at the intersections of the lattice points using Equation 1.

$$A_{F,K}^q(j) = - \sum_{i=1}^n W_{probe,k} W_{ik} e^{-a r_{iq}^2} \quad (1)$$

Where  $q$  represents a grid point,  $i$  is the summation index over all atoms of the molecule  $j$  under computation,  $W_{ik}$  is the actual value of the physicochemical property  $k$  of atom  $i$ , and  $W_{probe,k}$  is the

value of the probe atom. In the present study, similarity indices were computed using a probe atom ( $W_{\text{probe},k}$ ) with charge +1, radius 1Å, hydrophobicity +1, and attenuation factor  $a$  of 0.3 for the Gaussian type distance. The statistical evaluation for the CoMSIA analyses was performed in the same way as described for CoMFA.

## PLS calculations and validations

Partial least-square (PLS) (Bush *et al.*, 1993) methodology was used for all 3D QSAR analyses. Column filtering was set to 2.0 kcal/mol to speed up the analysis and reduce the noise. The CoMFA and CoMSIA descriptors were used as independent variables, and  $\text{pIC}_{50}$  values were used as dependent variables in partial least-squares regression analyses to derive 3D QSAR models using the standard implementation in the SYBYL package. The predictive value of the models was evaluated first by leave-one-out (LOO) (Cramer *et al.*, 1988; Wold *et al.*, 1978) cross-validation. The cross-validated coefficient,  $q^2$ , was calculated using eq 2.

$$q^2 = 1 - \frac{\sum (Y_{\text{predicted}} - Y_{\text{observed}})^2}{\sum (Y_{\text{observed}} - Y_{\text{mean}})^2} \quad (2)$$

Where  $Y_{\text{predicted}}$ ,  $Y_{\text{observed}}$  and  $Y_{\text{mean}}$  are predicted, actual, and mean values of the target property ( $\text{pIC}_{50}$ ), respectively.  $\sum (Y_{\text{predicted}} - Y_{\text{observed}})^2$  is the predictive sum of squares (PRESS). To maintain the optimum number of PLS components and minimize the tendency to over fit the data, the number of components corresponding to the lowest PRESS value was used for deriving the final PLS regression models. In addition to the  $q^2$  and number of components, the conventional correlation coefficient  $r^2$  and its standard error  $s$  (SEE) were also computed. The models gave satisfactory LOO crossvalidated  $q^2$  value of 0.580 and 0.610 and conventional  $r^2$  value of more than 0.949 and 0.949 for CoMFA and CoMSIA respectively, indicating their good predictive ability.

## Hardware and Software

InsightII 2000.1 and Sybyl 7.1 were used for molecular modeling on a SGI Origin 300 workstation equipped with 4 \* 600 Mhz R12000 processors.

## RESULTS

CoMFA and CoMSIA 3D-QSAR models were derived using a series of xanthone derivatives as potent alpha glucosidase inhibitors. The predictive power of the 3D-QSAR models derived using training set were assessed by predicting biological activities of the test set molecules. The CoMFA and CoMSIA 3D-QSAR methods are based on the assumption that the changes in binding affinities of ligands are related to changes in molecular properties represented by fields. The

alignment rule and the bioactive conformation are crucial variables in any 3D-QSAR analysis as both will affect outcome of statistical analysis. The further alignment of compounds based on docked conformation of most active compound 28, Fig. 1 was considered in the study. This was done in order to rule out probability of any uneven conformations obtained sometimes in case of top conformations of docked ligands. Hence alignment was then done on the best scoring conformation of most active ligand. The core and the aligned compounds are shown in Fig. 2.

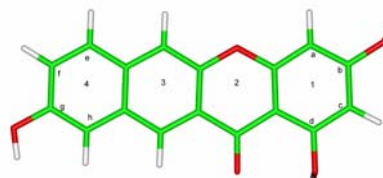


Figure 1: Docked conformation of compound 28.

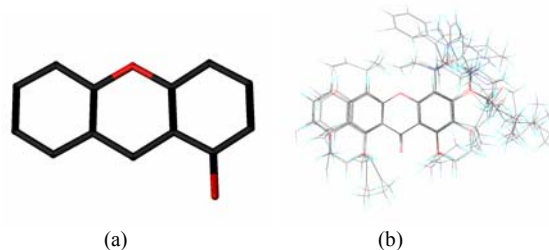


Figure 2: (a): Substructure used for alignment (b) Alignment of compounds.

## CoMFA 3D-QSAR analysis

Steric and electrostatic CoMFA fields were generated using standard procedures (Clark *et al.*, 1990). CoMFA model based on molecular docking and database alignments was considered for analysis. The statistical details and actual and predicted  $\text{pIC}_{50}$  values of the training and test sets are summarized in Table 2 [Supplementary data].

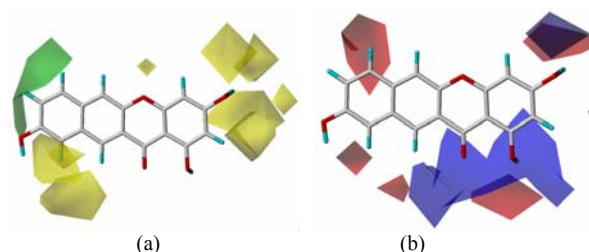
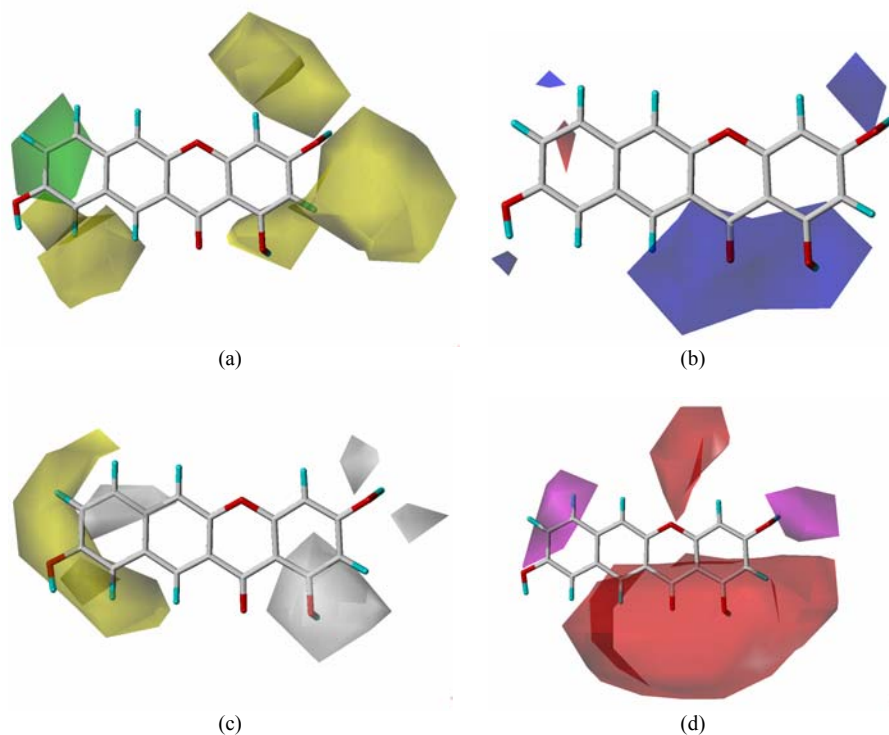


Figure 3: Compound 28 mapped on (a) CoMFA steric (b) electrostatic contour.

The CoMFA steric and electrostatic field contour plots obtained from the dual alignment procedure are shown



**Figure 4:** Compound 28 mapped on CoMSIA (a) steric (b) electrostatic (c) hydrophobic and (d) hydrogen acceptor contour maps.

in Fig. 3. The steric interactions are represented by green- and yellow-colored contours, while electrostatic interactions are represented by red- and blue-colored contours. In the green regions of steric contour plot, bulky substituents enhance biological activity, while bulky substituents in the yellow regions are likely to decrease activity. Blue-colored contours represent regions where electropositive groups increase activity, whereas red-colored regions represent areas where electronegative groups enhance activity.

The green steric contour on left side near ring 4 indicates that any bulkier substituent is preferred at this position Fig. 3a. Thus, molecules which either carry a 4th benzene ring or bulkier substituents such as alkyl, hydroxyl groups attached to the 3<sup>rd</sup> ring (12, 27-32, 36, 41) are more active than compounds without such substitutions (1-6, 21, 24). Hence addition of bulky groups like hydroxyl, alkyl or benzyl groups on left side near the sole green contour might aid in improving potency of inhibitors. Moderate activity of 38 is due to the presence of terminal alkyl group attached to ring 3 occupying the yellow contour region on the left side. Another group of sterically disfavored yellow contours are present at the right side. Compounds having bulky substituents at this position are hence less active, for example low potency of most compounds (15-19, 21, 23-25, 37) might be attributed to the presence of substitutions attached to ring1 at these yellow contours. This indicates that removal of bulky groups from ring1 will enhance the activity of these compounds.

The CoMFA electrostatic contour plot is shown in Fig. 3b. The red regions near position e and h of ring 4 indicate that any electronegative group at this position would enhance the activity. Therefore 29 in which the O atom of -OH group attached to fourth ring is more active than 1, 3-6, 10, 13-19, 23 and 26 wherein no such group is attached. Hence, substitution of electronegative group at these red contours near ring 4 will enhance the activity of compounds. The blue contour surrounding lower portion of rings 1, 2 and 3 indicate that substitution of electropositive group at this position would increase the activity. Hence, 7, 8, 27- 29, 32 and 37 with -OH groups on ring1 pointing towards this blue contour have higher potency than compounds 1, 4, 10 26 and 42, which either

lack any electropositive group or in which it is farther from it. However, the =O group attached on ring2 near the blue contour in most of the compounds must be substituted by some electropositive group in order to increase the activity. Presence of blue contour at upwards right position to ring1 determines that the electropositive environment is desirable at this position, hence electropositive -OH group occupying this position is present in all potent compounds like 8, 28-29, 31 and 32.

### CoMSIA 3D-QSAR analysis

The CoMSIA method defines explicit hydrophobic (H) and hydrogen bond donor (D) and acceptor (A) descriptors in addition to the steric (S) and electrostatic (E) fields used in CoMFA. PLS analyses of CoMSIA model obtained is shown in Table 2. The CoMSIA model including S, E, H, and A fields gave the highest value in PLS analysis.

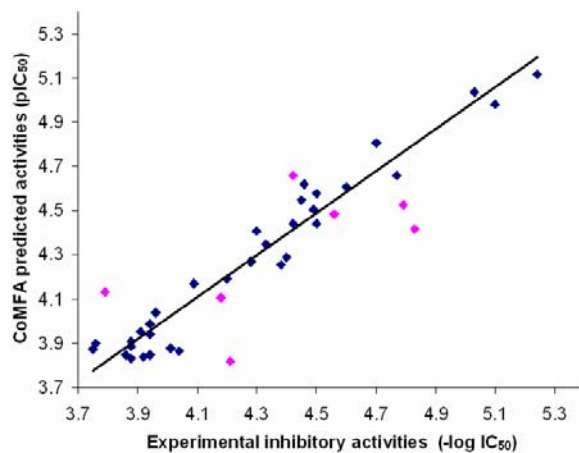
In CoMSIA method, the steric fields are represented by green- and yellow-colored contours (green, bulky substitution favored; yellow, bulky substitution disfavored); the electrostatic fields are indicated by red- and blue-colored contours (blue, electropositive group favored; red, electronegative group favored); the hydrophobic fields represented by yellow- and white-colored contours (yellow, favored; white, disfavored); the hydrogen bond donor fields are indicated by cyan- and purple-colored contours (cyan, favored; purple,

disfavored); while the hydrogen bond acceptor fields are denoted by magenta and red contours (magenta, favored; red, disfavored).

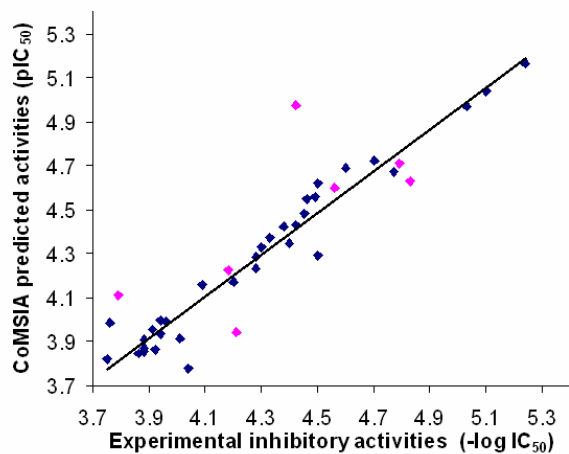
The CoMSIA contour plots employing S, E, H, and A fields are shown in Fig. 4. The steric and electrostatic plot (Fig. 4a & b) are more or less similar to the corresponding CoMFA plots except that there is an absence of some red contours in CoMSIA electrostatic contour map on the left side. The hydrophobic and hydrogen bond acceptor contours are shown in Fig. 4c & d respectively. The big yellow hydrophobic contour elliptically surrounding the ring 4 (Fig. 4c) matches with the green steric contour in Fig. 3a. This indicates that any bulky group with lipophilic character is preferred at this position. Similarly the sterically disfavored yellow contours match with hydrophobically disfavored white regions in areas surrounding ring1, indicating that bulky substituents especially lipophilic ones are strictly disfavored at this position. The high potency of compounds 27- 33 is due to the reason that some part of their ring4 is embedded in the hydrophobically favored yellow contour. Similarly 11, 36 and 38 are more active as the methyl groups substituted on ring 3 are embedded in yellow contour. The comparatively lesser activity of 9 and 34 is due to the presence of methyl and phenyl group at position d of ring1 near the white contours on right side. Again, compounds like 10, 15-19, 21-24 and 25 are still less potent as most of their ring 1 substituents at position b occupy the white contour. Lesser activity of 37, 40, 41 and 42 is due to the occurrence of their substituents at either position a or b or both at ring1 near the white contour. The slightly lesser activity of 38 than 28 is due to the presence of its alkyl substituent on position a of ring 1 in white contour. The medium potency of 11, 12, 36 is due to the presence of their alkyl substituents on ring 3 in the yellow region and at the same time presence of their alkyl substituents at position b or position d of ring 1 in white contours. Hence it is assumed that hydrophobic groups attached to ring 1 are responsible for lower potency of these compounds.

The acceptor contour map is characterized by a red and magenta contours Fig. 4d. The big red contour below indicating hydrogen bond donor favored area matches with the electropositively favored blue region of electrostatic contour [Fig. 3b]. Hence electropositive hydrogen bond donor groups are extremely favored at this position. The presence of -OCH<sub>3</sub> on ring 3 in this red contour is responsible for low activity of compound 10. The slightly better activity of 22 and 25 is due to the presence of their epoxide and tetrahydrofuran oxygens on ring 1 in right magenta contour responsible for acceptor favorable field; however 13-19 and 23 are less active due to absence of any such group in this contour. The high activity of 28 and 29 is due to the presence of -O of -OH group on ring4 near the acceptor favored magenta contour along with the

presence of -OH group in ring1 at the right red contour. Moderate activity of 3 and 5 is due to the presence of two -OH groups in ring 1 and 3 in red contours which is favorable for hydrogen donors. The various O carrying substituents on ring1 like benzopyran, benzofuran ring, methoxy group etc embedded in magenta contour accounting for better potency of 8, 34, 39, 41 and 42. Again, moderately better activity of 30 is due to absence of =O from ring2 in red contour as compared to 1, 2, 4, 6, 20, 21, 26 and 35.



(a)



(b)

**Figure 5:** (a) CoMFA and (b) CoMSIA predicted activities (pIC<sub>50</sub>) vs the experimental activities (-logIC<sub>50</sub>) of training (■) and testing set (●) compounds.

## CoMFA versus CoMSIA

The predictive power of CoMFA and CoMSIA 3D-QSAR models were evaluated by using the test set of 8 molecules. In both models, the predictive values fall close to the actual pIC<sub>50</sub> values, not deviating by more than 1 logarithmic unit (Fig. 5, Table 1) in most of the cases. Both models predicted higher (pIC<sub>50</sub>) activity for the most active compound 28 of the series complementing its actual activity (IC<sub>50</sub>). In summary, the differences between CoMFA and CoMSIA are not striking and both models demonstrated good predictive ability.

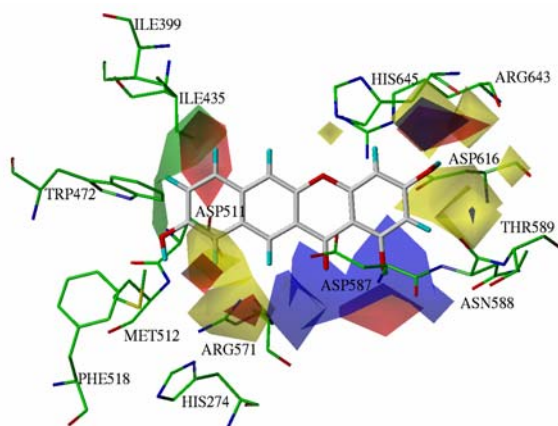


**Figure 6:** CoMFA steric and electrostatic contours mapped on active site.

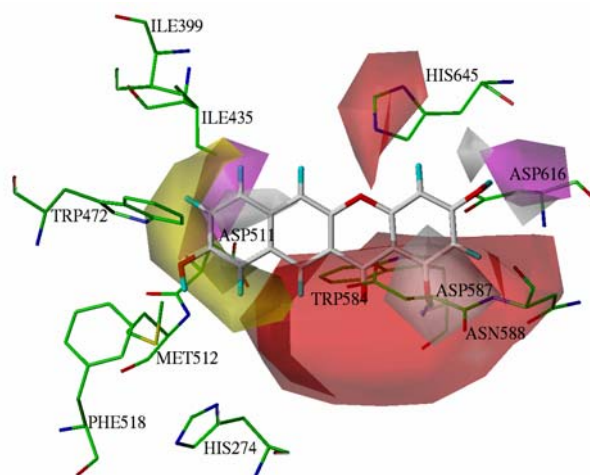


**Figure 7:** CoMSIA hydrophobic and hydrogen bond acceptor contours mapped on active site.

### Receptor topology and contour map correlation

The CoMFA steric contour mapped on receptor active site is shown in Fig. 6. The bulk favoring contour (green colored) is seen around residues Ile399, Ile435 and Trp472. On the other hand, bulk disfavoring interactions as indicated by the smaller yellow colored contours at the left side, line the pocket composed of Asp511, Met512, His274, Arg571. Whereas, the smaller cluster of yellow contours on the right side are occupied and delineated by various charged bulky groups like Asn588, Asp616, Arg643, and His645. In the context of electrostatic interactions, the electropositively favored big blue contour near ring4 is occupied by the electronegative Asp587. The blue contour near His645 is justified by the presence of electron withdrawing nitrogens on histidine. The electronegatively favored red region occupying the Arg571 residue is justified due to the electropositive nature of arginine nitrogens.

CoMSIA provides additional information over CoMFA in terms of hydrogen bonding and hydrophobic interactions with the receptor, Fig. 7. CoMSIA contours indicating hydrogen bond acceptor aptitudes are seen in the proximity of Asp511, Asp587, Trp584, Asp398 and His645. Specially the hydrogen donor favored red contour below occupied by Asp587 and Asp511 is justified because of acceptor oxygen on them. Similarly, another red contour present above the plane of compound 28 is occupied by His645 due to the acceptor properties of histidine nitrogens. Contours favoring hydrophobic interactions (yellow color) are seen near Ile399, Ile435, Trp472, Met512, Phe518, while disfavored hydrophobic interactions (white color) lie in the pocket made by Asp 511, Asp587, Asn588 and Asp616. The hydrophobic (Phe,Ile,Trp,Met) and polar (Asp, His, Asn ) nature of these residues are in line with the character of the contours.

### CONCLUSION

The QSAR analysis provides useful insights into the structural features that may be appended to the basic pharmacophore of the alpha glucosidase inhibitors so as to improve their potency. The dual, docking as well as common substructure based alignment in the present case gave a better picture of the bioactive conformations that these diverse inhibitors adopt within the alpha glucosidase active site. A comparison of the 3D-QSAR field contributions with the structural features of the binding site showed good correlation between the two analyses. To our knowledge, this is the first study aimed at deriving predictive 3D-QSAR models for alpha glucosidase inhibitors. This information will be useful in the design of novel anti-diabetic drug candidates.

### Acknowledgement

This manuscript is CDRI communication number 7607. This work was supported by the Council of Scientific and Industrial Research (CSIR) funded network project CMM0017- Drug Target development using in silico biology. US thank CSIR for fellowship.

### References

- Boehringer Ingelheim (2007) Annual Report. Page: 38.
- Braun C, Brayer GD *et al.* (1995) Mechanism-based inhibition of yeast alpha-glucosidase and human pancreatic alpha-amylase by a new class of inhibitors, 2-Deoxy-2,2-difluoro-alpha-glycosides. *J. Biol. Chem.* **270**(45):26778–26781.
- Bush BL, Nachbar RB Jr. (1993) Sample-distance Partial Least Squares: PLS optimized for many variables, with application to CoMFA. *J. Comput. Aided Mol. Des.* **7**(5):587-619.

- Cho SJ, Tropsha A (1995) Cross-validated  $R^2$ -guided region selection for comparative molecular field analysis: a simple method to achieve consistent results. *J. Med. Chem.* **38**:1060–1066.
- Clark M, Cramer III RD, *et al.* (1989) Validation of the general purpose tripos 5. 2 force field. *J. Comput. Chem.* **10**:982–1012.
- Clark M, Cramer III RD, *et al.* (1990) Comparative molecular field analysis (CoMFA) Toward its use with 3D structural databases. *Tetrahedron Comput. Methodol.* **3**: 47–59.
- Cramer RD, Patterson DE, *et al.* (1988) Comparative molecular-field analysis (CoMFA). 1. Effect of shape on binding of steroids to carrier proteins. *J. Am. Chem. Soc.* **110**:5959–5967.
- Cramer RD, Bunce JD, *et al.* (1988) Crossvalidation, Bootstrapping, and Partial Least Squares Compared with Multiple Regression in Conventional QSAR Studies. *Quant Struct Act Relat.* **7**: 18-25.
- Das SK, Chakrabarti R (2005) Non-Insulin Dependent Diabetes Mellitus: Present Therapies and New Drug Targets. *Mini Reviews in Medicinal Chemistry* **5**(11):1019- 1034.
- Dwek RA, Butters TD, *et al.* (2002) Targetting glycosylation as a therapeutic approach. *Nat. Rev. Drug Disc.* **1**:65–75.
- Gao H, Kawabata J (2005)  $\alpha$ -Glucosidase inhibition of 6-hydroxyflavones. Part 3: Synthesis and evaluation of 2,3,4-trihydroxybenzoyl-containing flavonoid analogs and 6-aminoflavones as  $\alpha$ -glucosidase inhibitors. *Bioorganic & Medicinal Chemistry* **13**(5):1661–1671.
- Gohlke H, Hendlich M, *et al.* (2000) Knowledge-based Scoring Function to Predict Protein-Ligand Interactions. *J. Mol. Biol.* **295**:337-356.
- Hai-Wei X, Gui-Fu D, *et al.* (2007) Synthesis of andrographolide derivatives: A new family of  $\alpha$ -glucosidase inhibitors. *Bioorganic & Medicinal Chemistry* **15**(12):4247–4255.
- Insight II 2000.1 Program (2000) Accelrys, San Diego, CA.
- International Diabetes Federation. Diabetes Atlas. 3rd edn. Brussels: International Diabetes Federation, 2006.
- Klebe G, Abraham U, *et al.* (1994) Molecular similarity indexes in a comparative-analysis (Comsia) of drug molecules to correlate and predict their biological-activity. *J. Med. Chem.* **37**(24): 4130–4146.
- Lajola FM, Filho JM, *et al.* (1984) Effect of a bean (*Phaseolus vulgaris*)  $\alpha$ -amylase inhibitor on starch utilization. *Nutrition Reports International.* **30**(1):45-54.
- Liu Y, Zou L, *et al.* (2006) Synthesis and pharmacological activities of xanthone derivatives as  $\alpha$ -glucosidase inhibitors. *Bioorganic & Medicinal Chemistry* **14**(16): 5683–5690.
- Liu Y, Ma L, *et al.* (2007) Synthesis of xanthone derivatives with extended  $\pi$ -systems as  $\alpha$ -glucosidase inhibitors: Insight into the probable binding mode. *Bioorganic & Medicinal Chemistry.* **5**(8): 2810–2814.
- Madariaga H, Lee PC, *et al.* (1998) Effects of graded alpha-glucosidase inhibition on sugar absorption in vivo. *Dig Dis And Sci.* **33**(8):1020-1024.
- Matsuura H, Miyazaki H, *et al.* (2004) Isolation of  $\alpha$ -glucosidase inhibitors from hyssop (*Hyssopus officinalis*). *Phytochemistry.* **65**(1):91–97.
- McCulloch DK, Kurtz AB *et al.* (1983) A new approach to the treatment of nocturnal hypoglycemia using alpha-glucosidase inhibition. *Diabetes Care* **6**(5):483-487.
- Melo E.B., Gomes A.S. *et al.* (2006).  $\alpha$ - and  $\beta$ -Glucosidase inhibitors: chemical structure and biological activity. *Tetrahedron.* **62**(44):10277–10302.
- Rarey M, Kramer B, *et al.* (1996) A fast flexible docking method using an incremental construction algorithm. *J. Mol. Biol.* **261**(3):470-89.
- Robinson KM, Begovic ME, *et al.* (1991) New potent  $\alpha$ -glucohydrolase inhibitor MDL 73945 with long duration of action in rats. *Diabetes* **40**(7):825-830.
- Saqib U, Siddiqi MI (2008) Probing ligand binding interactions of human alpha glucosidase by homology modeling and molecular docking. *International Journal of Integrative Biology.* **2**(2):116-121.
- Seo EJ, Curtis-Long MJ, *et al.* (2007) Xanthones from *Cudrania Tricuspidata* displaying potent  $\alpha$ -glucosidase inhibition. *Bioorganic & Medicinal Chemistry Letters* **17**:6421–6424.
- Stahle L, Wold S, *et al.* (1988) Multivariate data analysis and experimental design in biomedical research. *Elsevier Science Publisher.* **25**:292–338.
- SYBYL Molecular Modeling System Version 7.1 (2005) Tripos Inc., St. Louis, MO.
- Truscheit E, Frommer W *et al.* (1981) Chemistry and Biochemistry of Microbial  $\alpha$ -Glucosidase Inhibitors. *Angew Chem Int. Ed Engl* **20**(9):744-761.
- Viswanadhan VN, Ghose AK, *et al.* (1989) *J. Chem. Inf. Comput. Sci.* **29**(3):163-172.
- Wold S (1978) Cross-validation estimation of the number of components in factor and principal components analysis. *Technometrics* **24**:397-405.
- World Health Organisation. Fact Sheet No. 312: What is Diabetes?. Available at: <http://www.who.int/mediacentre/factsheets/fs312/en/>.